Automatic Onset Detection of Abnormal Ventricular Potentials by Time-Frequency Analysis

Marco Orrù[1,2,§], Nicla Mandas[3,2,§], Giulia Baldazzi[2], Graziana Viola[4], Danilo Pani[2]

[1] Department of Informatics, Bioengineering, Robotics and Systems Engineering (DIBRIS), University of Genova, Genova, Italy
[2]Department of Electrical and Electronic Engineering (DIEE), University of Cagliari, Cagliari, Italy
[3]The Hadron Academy, Istituto Universitario di Studi Superiori, IUSS, Pavia, Italy
[4]Cardiology Unit (UTIC), Santissima Trinità Hospital, Cagliari, Italy

Abstract

Activation times in intracardiac electrograms (EGMs) may help clinicians in detecting abnormal pathways sustaining post-ischemic ventricular tachycardia (VT). As they are especially accurate when estimated only from the near-field component of abnormal ventricular potentials (AVPs), this work proposes a novel approach for AVP onset identification, leveraging the Hilbert-Huang Transform (HHT) and a knee-point detection technique.

A dataset composed of 940 delineated AVPs was used. The HHT was exploited to compute an expedient signal as the product between the instantaneous frequency and energy, only when the frequency fell within a specific range. Values ranging from 0 to 490 Hz were tested for the lower limit, while the upper limit was fixed to 500 Hz. On the expedient signal, the cumulative area is computed, and the AVP onset was identified as its knee-point.

Based on the absolute errors distributions and the percentage of errors lower than 10 ms, the optimal lower frequency threshold resulted in 110 Hz, with a median error in the onset delineation of 13.5 ms.

This approach could be relevant for electrophysiological studies aimed at VT suppression, by enabling the identification of near-field components in AVPs, and a more accurate assessment of their local activation timing.

1. Introduction

During cardiac electrophysiological studies, intracardiac electrograms (EGMs) are generally characterized by their own local activation time (LAT), considered as the time of activation of the EGM, referenced to a fiducial point detected on the surface ECG (e.g., the R peak). In the case of post-ischemic ventricular tachycardia (VT), the pathological EGMs recorded in the substrate sustaining the arrhythmia, i.e., abnormal ventricular potentials (AVPs), present altered LATs. Indeed, the damaged areas of the myocardium can cause a slowing down of the electrical conduction, which reflects the occurrence of delayed EGMs. Hence, this latency is of interest during transcatheter ablation procedures to properly identify arrhythmogenic areas and their conduction pathways. In the literature, several definitions of EGM activation have been described to compute the LAT. For instance, a study focused on investigating the optimal LAT annotation approach to better understand and characterize the abnormal conduction pathways [1]. Other studies [2], [3] proposed algorithms for identifying both the onset and end of the EGMs, but without taking into account the difference between its far-field and near-field components. This distinction has a key role in AVPs characterization, where isolating the pathological near-field activation allows for a more accurate LAT definition, related to the arrhythmogenic substrate.

In this explorative study, we introduce a novel approach for the characterization of AVPs, aimed at precisely delineating their onset within the EGM. Unlike previous studies, our method focuses specifically on the local near-field activation within the pathological component of the signal. Specifically, the EGM time-frequency dynamics were extracted using the Hilbert-Huang Transform (HHT), and the AVP onset was detected through a knee-point technique. This strategy allows for a precise description of the conduction delay intrinsic to the arrhythmogenic substrate.

2. Materials and methods

This study exploits the ARGO dataset, previously presented in detail in [4]. It comprises intracardiac EGMs recorded from nine patients with post-ischemic

§ These authors equally contributed to this work.

ventricular tachycardia who underwent radiofrequency catheter ablation. Recordings were collected during sinus rhythm following a standard electroanatomical mapping and ablation protocol.

The full dataset includes 1962 EGMs, categorized into one of three classes: physiological EGMs, AVPs, and unknown. Given the objective of this work, only the 940 signals labeled as AVPs were considered. For each signal labeled as AVP, the dataset provides the onset of the pathological event, derived from the consensus of three experts, which has been used in the subsequent analysis as ground truth.

2.1. Onset delineation algorithm

Firstly, each EGM has been preprocessed by taking a 500 ms window around the reference annotation, to extract the segment of the signal for which we are certain of the reliability of the acquisition (electrode in contact, adequate contact force of the catheter, etc.). The delineation method takes inspiration from the Simultaneous Amplitude Frequency Electrogram Transformation (SAFE-T) [5] algorithm and starts by applying the Empirical Mode Decomposition to each EGM. From this decomposition, only the first Intrinsic Mode Function (IMF) was kept and used to compute the Hilbert-Huang spectrum by applying the HHT.

In line with the SAFE-T approach, an expedient signal was computed by multiplying the instantaneous frequency and energy, elementwise. The SAFE-T metric, already used in prior studies [5] for identifying VT isthmuses, was revised here to highlight AVP onset in pathological EGMs. To this aim, only a frequency constraint was introduced to guide the analysis: indeed, a product signal was computed only when the instantaneous frequency fell within a selected range; otherwise, it was set to zero. To investigate which portions of the frequency spectrum were most informative for detecting the onset, all possible sub-bands ending at 500 Hz were explored. Specifically, the lower cutoff frequency was varied from 0 Hz to 490 Hz in 10 Hz steps, generating a series of frequency bands that progressively narrowed toward the upper end of the spectrum. This approach allowed to assess how different ranges of the frequency content contributed to the identification of the onset.

From the resulting signal, its cumulative area was computed. Such a curve was then normalized by the total area, producing a smooth, monotonically increasing function between 0 and 1. This curve had a typical sigmoid shape, which made it possible to capture the timing of the activation by a further processing step. Hence, the onset point was defined as the inflection point of this sigmoid (i.e., its knee), which was identified automatically using the Kneedle algorithm [6]. The

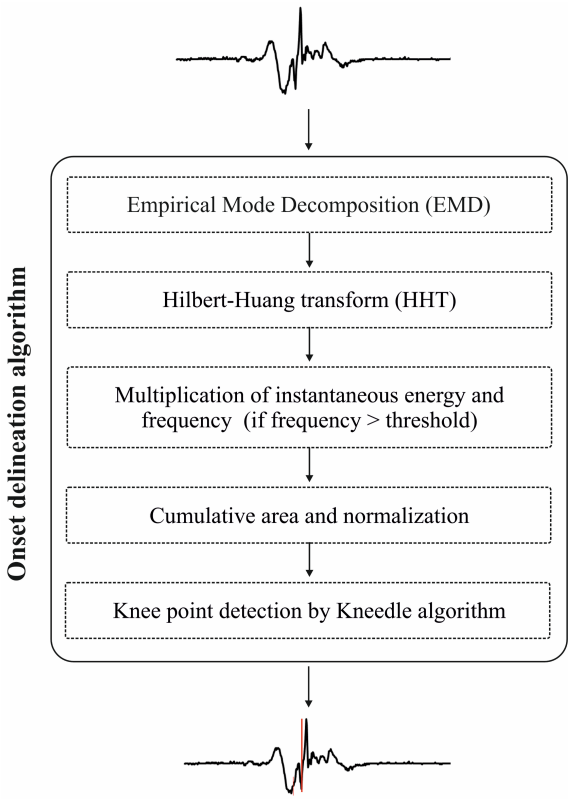

Figure 1. Overview of the processing pipeline for AVP onset detection. An example of an AVP trace is represented in the figure, while the red line indicates the onset predicted by the algorithm.

Kneedle algorithm was used as it finds the knee of a monotonic curve marking a sudden change in its trend. Whenever the algorithm couldn't detect a knee point on the curve, then the onset was set to a default out-of-range value (i.e., −1000). **Fig. 1** provides a step-by-step overview of the entire processing pipeline described above.

2.2. Performance evaluation

To evaluate the performance of the proposed algorithm, the error was computed as the difference between the ground truth of the AVP onset and the resulting one from the Knee point detection. After the first error analysis, among the tested frequency values, a narrow range was taken under consideration for the subsequent analysis, as the one that gave the lowest median absolute error. On this restricted set of ranges, the percentage of absolute errors under 5, 10, and 15 ms, inspired by [7], as well as the Pearson's correlation coefficient. Once the optimal frequency value was chosen, a linear regression analysis between the ground truth and the predicted AVP onsets was discussed.

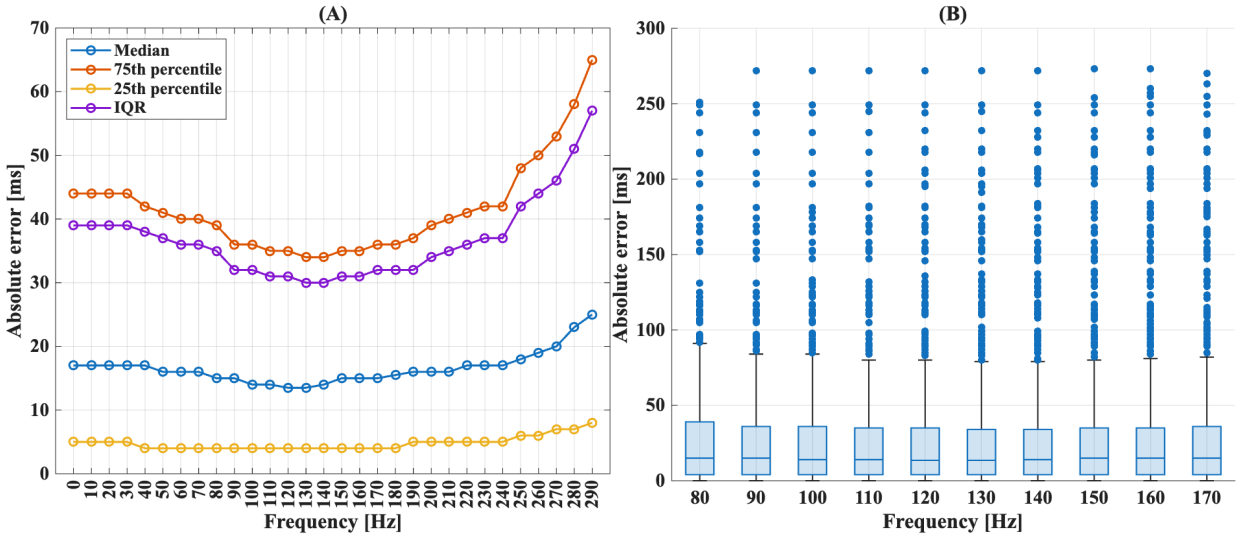

Figure 2. (A) Absolute onset detection error across lower frequency thresholds from 0 to 290 Hz. Median, 25th and 75th percentiles, and IQR are shown. (B) Boxplots of absolute detection error across the frequency thresholds from 80 to 170 Hz.

3. Results and discussion

Fig. 2A shows the median, 25th and 75th percentiles, as well as the interquartile range (IQR) of the absolute error, for the frequency threshold varying from 0 up to 290 Hz. Notably, beyond this upper limit (i.e., 290 Hz), the algorithm shows a progressive degradation in onset detection, with more frequent failures resulting in default out-of-range outputs. Hence, the distribution of absolute errors widens significantly, leading to markedly higher median values. Given the increasing error trend, results beyond 290 Hz are omitted for the sake of clarity. From this figure, the region in which the lower limit varies from 80 to 170 Hz was selected for the subsequent analysis, as it is characterized by the lowest median absolute errors (i.e., between 13.5 and 15 ms) and IQRs (i.e., between 30 and 35 ms). **Fig. 2B** shows in detail the boxplot for the selected frequency range. **Fig. 3** presents a stacked bar plot illustrating the percentage of absolute onset detection errors across the tested frequency thresholds. As shown, the range between 110 and 130 Hz yields the highest percentage of detections with an error below 15 ms, indicating these values as potential candidates for the optimal frequency threshold. However, when also considering the proportion of more accurate detections, i.e., those with errors under 5 ms and 10 ms, the best performance is obtained at 110 Hz, with a median absolute error equal to 13.5 ms. Moreover, by also looking at the Pearson's correlation coefficients reported in **Fig. 4**, the selection of 110 Hz yields a high correlation between predicted and ground truth AVP onsets (about 0.63). For this optimal threshold value, a regression analysis was performed (see **Fig. 5**). From this figure, a positive correlation can be seen between the predicted onsets and the ground truth annotations, indicating that

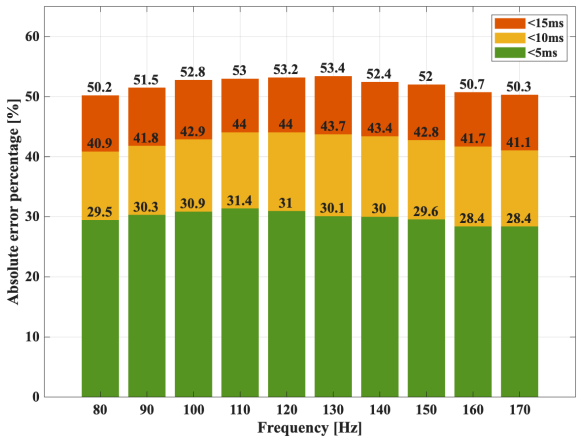

Figure 3. Stacked bar plot of absolute onset detection errors percentages across frequency thresholds from 80 to 170 Hz.

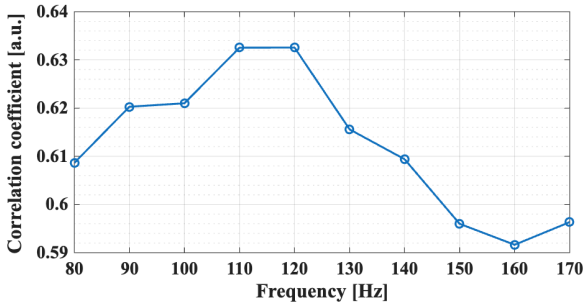

Figure 4. Pearson's correlation coefficient between the predicted and ground truth AVP onset times, across frequency thresholds from 80 to 170 Hz.

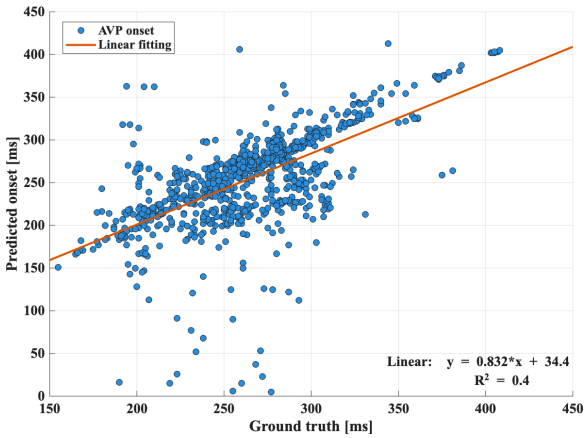

Figure 5. Scatter plot comparing predicted and ground truth AVP onset times, considering the optimal lower frequency limit. The linear fit (red) shows a moderate correlation ($R^2 = 0.40$)

the algorithm tends to properly detect the onset in most cases. However, the dispersion of the points in the lower ground-truth range (i.e., under 300 ms) suggests the tendency of the approach to underestimate the onset. These deviations influence the correlation coefficient by introducing significant variance that moves the fit away from the ideal one.

4. Conclusions

This study proposed a fully automated method for the onset delineation of AVPs, exploiting time-frequency decomposition through the HHT and a knee-point detection algorithm. The approach focused specifically on identifying the near-field activation within AVPs, instead of estimating a global LAT for the entire EGM.

Optimal performance was achieved when selecting all the frequencies above 110 Hz, with a good agreement with the ground truth annotations. The onset delineation was affected by a median absolute error of 13.5 ms. A positive correlation with the ground truth was observed.

This framework might be a valuable tool for substrate characterization in post-ischemic VT. In future work, this strategy could be extended to support not only the identification of the onset of the AVPs, but also their end, thus enabling a full assessment of pathological near-field duration. Moreover, alternative time-frequency transforms could be explored to further enhance robustness and precision in the explored task.

Acknowledgments

This work was carried out in the framework of the Ablation Reinforcement by computer-aided Guidance and Optimization (ARGO) study, approved by Azienda Tutela Salute Sardegna (ATS Sardegna). The research leading to these results has received funding from the European Union - NextGenerationEU through the Italian Ministry of University and Research under PNRR - M4C2-I1.3 Project PE_00000019 "HEAL ITALIA" to G. B., CUP F53C22000750006. The views and opinions expressed are those of the authors only and do not necessarily reflect those of the European Union or the European Commission. Neither the European Union nor the European Commission can be held responsible for them.

References

[1] J. Hawson *et al.*, "Optimal annotation of local activation time in ventricular tachycardia substrate mapping," *Clinical Electrophysiology*, vol. 10, no. 2, pp. 206–218, 2024.

[2] M. Masjedi *et al.*, "A novel algorithm for 3-D visualization of electrogram duration for substrate-mapping in patients with ischemic heart disease and ventricular tachycardia," *PLoS One*, vol. 16, no. 7, p. e0254683, 2021.

[3] A. Alcaine *et al.*, "A wavelet-based electrogram onset delineator for automatic ventricular activation mapping," *IEEE Trans Biomed Eng*, vol. 61, no. 12, pp. 2830–2839, 2014.

[4] M. Orrú *et al.*, "Introducing the ARGO Dataset of Post-Ischemic Ventricular Tachycardia Bipolar Electrograms," in *2023 Computing in Cardiology (CinC)*, IEEE, 2023, pp. 1–4.

[5] C.-Y. Lin *et al.*, "Simultaneous Amplitude Frequency Electrogram Transformation (SAFE-T) Mapping to Identify Ventricular Tachycardia Arrhythmogenic Potentials in Sinus Rhythm," *JACC Clin Electrophysiol*, vol. 2, no. 4, pp. 459–470, 2016.

[6] V. Satopaa, J. Albrecht, D. Irwin, and B. Raghavan, "Finding a 'kneedle' in a haystack: Detecting knee points in system behavior," in *2011 31st International Conference on Distributed Computing Systems Workshops*, IEEE, 2011, pp. 166–171.

[7] M. El Haddad, R. Houben, R. Stroobandt, F. Van Heuverswyn, R. Tavernier, and M. Duytschaever, "Algorithmic detection of the beginning and end of bipolar electrograms: implications for novel methods to assess local activation time during atrial tachycardia," *Biomed Signal Process Control*, vol. 8, no. 6, pp. 981–991, 2013.

Address for correspondence:

Nicla Mandas
Istituto Universitario di Studi Superiori, IUSS, Pavia, Italy
MeDSP Lab, Department of Electrical and Electronic Engineering, University of Cagliari, Italy
nicla.mandas@iusspavia.it